MOUNTAIN-PLAINS CONSORTIUM

MPC 22-491 | A. L. Breverman and J. D. Niemann

EVALUATING NONLINEAR METHODS TO GENERATE FLOOD HYDROGRAPHS FOR BRIDGE SCOUR APPLICATIONS

MOUNTAIN-PLAINS CONSORTIUM REGION 8

A University Transportation Center sponsored by the U.S. Department of Transportation serving the Mountain-Plains Region. Consortium members:

Colorado State University
North Dakota State University
South Dakota State University
University of Colorado Denver
University of Denver
University of Utah
Utah State University
University of Wyoming

Technical Report Documentation Page

1. Report No.	2. Government Accession No.	3. Recipient's Catalog No.
MPC-619		

4. Title and Subtitle	5. Report Date
Evaluating Nonlinear Methods to Generate Flood Hydrographs for Bridge Scour Applications	December 2022
	6. Performing Organization Code

7. Author(s)	8. Performing Organization Report No.
Avital L. Breverman and Jeffrey D. Niemann	MPC 22-491

9. Performing Organization Name and Address	10. Work Unit No. (TRAIS)
Colorado State University Campus Delivery 1372 Fort Collins, CO 80523	11. Contract or Grant No.

12. Sponsoring Agency Name and Address	13. Type of Report and Period Covered
Mountain-Plains Consortium North Dakota State University PO Box 6050, Fargo, ND 58108	Final Report
	14. Sponsoring Agency Code

15. Supplementary Notes

Supported by a grant from the US DOT, University Transportation Centers Program

16. Abstract

Bridge scour evaluations are often performed using streamflow estimates from regional regression relationships. This approach relies on the accuracy of the relationships and does not consider the effects of flow variations. Alternatively, a complete hydrograph can be obtained from a watershed model and used in the scour analysis. However, hydrograph estimation is complicated by nonlinearities in basin response, particularly when large storm events are considered. The objective of this study was to determine whether nonlinearities in hydrologic response and the relationship between flow rates and scour can substantially impact bridge scour evaluations. Nonlinearity in the relationship between excess precipitation and direct runoff was included using variable Clark unit hydrograph parameters in a HEC-HMS model. Flow depths and velocities were then generated using a two-dimensional HEC-RAS model. Both models were developed for the Cheyenne Creek watershed west of Colorado Springs. Anticipated scour was quantified using approaches detailed in the Federal Highway Administration's Hydraulic Engineering Circular manuals. Regression-based peak flow estimates applied as steady state discharges produced larger scour depths than unsteady hydrographs obtained from the hydrologic models. The hydrographs simulated using the variable Clark unit hydrograph parameters produced substantially larger scour depths than those simulated using constant Clark unit hydrograph parameters.

17. Key Word	18. Distribution Statement
bridges, flood hydrographs, guidelines, scour, streamflow	Public distribution

19. Security Classif. (of this report)	20. Security Classif. (of this page)	21. No. of Pages	22. Price
Unclassified	Unclassified	32	n/a

Evaluating Nonlinear Methods to Generate Flood Hydrographs for Bridge Scour Applications

Avital L. Breverman
Jeffrey D. Niemann (PI)

Department of Civil and Environmental Engineering
Colorado State University
Fort Collins, CO 80523

December 2022

Acknowledgments

The authors thank the Mountain-Plains Consortium and Colorado State University (CSU) for providing funds that made this study possible.

Disclaimer

The contents of this report reflect the views of the authors, who are responsible for the facts and the accuracy of the information presented. This document is disseminated under the sponsorship of the Department of Transportation, University Transportation Centers Program, in the interest of information exchange. The U.S. Government assumes no liability for the contents or use thereof.

ABSTRACT

Bridge scour evaluations are often performed using streamflow estimates from regional regression relationships. This approach relies on the accuracy of the relationships and does not consider the effects of flow variations. Alternatively, a complete hydrograph can be obtained from a watershed model and used in the scour analysis. However, hydrograph estimation is complicated by nonlinearities in basin response, particularly when large storm events are considered. The objective of this study was to determine whether nonlinearities in hydrologic response and the relationship between flow rates and scour can substantially impact bridge scour evaluations. Nonlinearity in the relationship between excess precipitation and direct runoff was included using variable Clark unit hydrograph parameters in a HEC-HMS model. Flow depths and velocities were then generated using a two-dimensional HEC-RAS model. Both models were developed for the Cheyenne Creek watershed west of Colorado Springs. Anticipated scour was quantified using approaches detailed in the Federal Highway Administration's Hydraulic Engineering Circular manuals. Regression-based peak flow estimates applied as steady state discharges produced larger scour depths than unsteady hydrographs obtained from the hydrologic models. The hydrographs simulated using the variable Clark unit hydrograph parameters produced substantially larger scour depths than those simulated using constant Clark unit hydrograph parameters.

TABLE OF CONTENTS

LIST OF TABLES

LIST OF FIGURES

1. INTRODUCTION

The most common cause of bridge failure in the United States is the erosion of streambed material from around bridge substructure elements (Federal Highway Administration, 2019). The collapse of the Schoharie Creek Bridge in New York state in April 1987 served as a catalyst for evaluation of bridge inspection and scour countermeasure design practices in the U.S. Three Federal Highway Administration (FHWA) Hydraulic Engineering Circular (HEC) manuals provide guidance for bridge scour and stream stability analyses: HEC-18 "Evaluating Scour at Bridges," HEC-20 "Stream Stability at Highway Structures," and HEC-23 "Bridge Scour and Stream Instability Countermeasures."

Evaluation of bridge scour is accomplished through the use of hydrologic events of a given recurrence interval, such as the 100-year flood (Clopper & Lagasse, 2011). These design storms are determined in one of three ways: (1) streamflow records from stream-gaging stations; (2) regional regression relationships based on characteristics such as drainage area, stream slope, land use, and mean annual precipitation (Capesius & Stephens, 2009); and (3) application of frequency-based design storm to a hydrologic model to determine runoff and ultimately streamflow.

For bridges located near a stream gage, the gage record length is often not long enough to perform a flow frequency analysis for scour design discharges. Regional regression relationships for frequency-based discharges are often used as an alternative to a site-specific flow frequency analysis. However, these relationships are not updated often enough to account for abrupt changes to watershed properties, such as wildfire impacts on soil infiltration properties. In addition, frequency-based estimates do not consider the streamflow production mechanism of a flood event and are provided as peak streamflow values.

Many bridges in the United States are not located near stream gages. As a result, streamflow data must be inferred from nearby gages or from hydrologic models. The Colorado Department of Transportation recommends the use of unit hydrograph (UH) theory in hydrologic models (Mommandi et al., 2004). A UH models the transformation of excess precipitation to runoff and is based on assumptions of time-invariance and superposition (Dooge, 1959). The superposition principle implies that the hydrograph resulting from a specific pattern of excess precipitation can be determined by superimposing the contributions from the individual excess rainfall units. However, calibrated unit hydrographs depend on the magnitude of the event under consideration.

Amorocho (1963) found that the response of laboratory catchments to a series of rainfall pulses exhibited a departure from the linearity assumption. Tromp-van Meerveld and McDonnell (2006a) studied nonlinearity resulting from the occurrence of threshold behavior in streamflow generation mechanisms. They observed a large increase in subsurface stormflow once precipitation exceeded a certain threshold. The "fill and spill hypothesis" postulates that subsurface stormflow enters the stream only when bedrock depression storage has been filled (Tromp-van Meerveld & McDonnell, 2006b). Another source of nonlinearity is the relationship between flow and flow speed. Lee and Yen (1997) used kinematic-wave theory to determine the travel times for overland and channel flow. They found that flow speed increased with larger discharges. Woolridge et al. (2020) investigated the response of watersheds in the Front Range of Colorado to large storm events. They found that the calibrated time of concentration decreases with increasing rainfall intensity, indicating different hydrologic responses to storms of varying magnitudes.

In this study, two nonlinearities in streamflow are investigated: (1) nonlinearity in the relationship between excess precipitation and direct runoff, and (2) nonlinearity in the relationship between streamflow and scour. The nonlinear response of watersheds has important implications for transportation infrastructure safety. Most streamflow events used for model calibration are typically much less intense than those required for scour design and analysis. Guidance from the Federal Energy Regulatory Commission cautions against the use of unit hydrographs developed from small floods for Probable

Maximum Flood inflow hydrographs (Federal Energy Regulatory Commission, 2001). It is common practice within the U.S. Army Corps of Engineers to increase the peak discharge of reservoir inflow unit hydrographs for dam safety studies by 25% to 50% to account for differences in watershed responses during large flood events (U.S. Army Corps of Engineers, 1991). The FHWA does not provide guidance on adjustment of unit hydrograph parameters for bridge scour design flows. Similarly, the nonlinear relationship between streamflow and scour suggests that the scour due to time varying streamflow rates may be different than the scour due to a steady average streamflow rate.

The objectives of this study are to investigate (1) the nonlinearity in the relationship between excess precipitation intensity and direct runoff, (2) the difference in computed scour depths resulting from the use of steady and unsteady discharge, and (3) whether these nonlinearities impact bridge scour evaluations. The study is performed for the Evans Avenue bridge over Cheyenne Creek west of Colorado Springs, Colorado. Woolridge et al. (2020) and Irvin (2021) developed hydrologic models and parameter estimation techniques for generation of design flows. The Clark method is used to estimate direct runoff from excess precipitation, and the parameter estimation techniques utilize the same Clark parameters for all precipitation intensities. The nonlinear relationship between excess precipitation intensity and streamflow is investigated using the variable parameter Clark method in the Hydrologic Engineering Center - Hydrologic Modeling System (HEC-HMS). Two independent estimates of frequency-based streamflow events are used to develop the variable parameters. A hydraulic model of Cheyenne Creek is developed using the Hydrologic Engineering Center - River Analysis System (HEC-RAS). Frequency-based peak discharges from regional regression equations and design storm hydrographs from the HEC-HMS models are applied to the hydraulic model. The resulting hydraulic variables (depth and velocity) are used to determine the extent to which steady and unsteady discharges differ in their computed bridge scour and the extent to which the constant and variable Clark methods affect scour. Contraction and pier scour depths are computed using equations from HEC-18.

The outline for this study is as follows. Section 2 discusses the study region. Section 3 discusses the modeling methods, including the previous hydrologic modeling efforts, the development of the variable Clark parameters, the hydraulic model structure, and the simulations. Section 4 presents the results of the hydrologic and hydraulic modeling. Section 5 discusses the conclusions of the study.

2. STUDY REGION

Cheyenne Creek is in central Colorado west of and within Colorado Springs. The creek is a tributary of Fountain Creek, which ultimately flows into the Arkansas River in Pueblo, Colorado. The Cheyenne Creek watershed, as delineated in this modeling effort, encompasses a drainage area of approximately 56 km^2 (Figure 2.1). The outlet of the Cheyenne Creek model is at USGS gage 07105490 Cheyenne Creek at Evans Avenue. Elevations in the Cheyenne Creek watershed range from 1,910 m in the vicinity of Evans Avenue to 3,650 m in the headwaters in the Rocky Mountains. Cheyenne Creek has two tributaries, which are North Cheyenne Creek and South Cheyenne Creek.

The Cheyenne Creek watershed was selected for analysis because a bridge carrying Evans Avenue over Cheyenne Creek is located adjacent to a United States Geological Survey (USGS) streamflow gage near the watershed outlet. Furthermore, the watershed has experienced multiple large floods during the period of record. The daily streamflow record at USGS gage 07105490 is shown in Figure 2.2. Woolridge et al. (2020) previously analyzed the active streamflow generation mechanisms during a mid-latitude cyclone (MLC) that affected Cheyenne Creek in 2013 and found that saturation-excess runoff and subsurface stormflow occurred. However, when considering synthetic design storms, they observed that infiltration-excess runoff can also occur.

Two water supply reservoirs, Mesa and Gold Camp, are located within the Cheyenne Creek watershed. The reservoirs are located north of North Cheyenne Creek, just upstream of the confluence with the main stem and near the watershed outlet. Water is diverted from both North and South Cheyenne Creeks, but the diversion structures did not operate during the June 1997 and September 2013 flood events along Cheyenne Creek (Colorado Department of Water Resources, n.d.). Two roadways, Evans Avenue and South Cheyenne Canyon Road, are carried over the mainstem Cheyenne Creek and North Cheyenne Creek, respectively, by bridges (Figure 2.3). The original Evans Avenue bridge was built in 1925 and replaced in 2016. The original bridge structure was selected for this scour analysis because it contained a pier within the stream. The Cheyenne Creek streambed is currently armored with riprap of approximately 1-m median diameter. Based on aerial imagery from 2018, riprap armoring extends approximately 30 m upstream of the bridge and 10 m downstream of the bridge.

Long-term streambed elevation changes in the vicinity of the Evans Avenue bridge were assessed through a specific gage analysis. Long-term aggradation and degradation may be the result of a natural or anthropogenic change to the stream or watershed (Federal Highway Administration, 2019). The specific gage analysis is a plot of the river stage that corresponds to a specific discharge over time (Biedenharn & Watson, 1997). Curves are plotted for discharges of varying magnitude to assess changes in the river's hydrologic regime (Blench, 1969). In general, an increase in stage for a given discharge indicates aggradation while a decrease in stage indicates degradation.

Approximately 400 field measurements (stage-discharge data pairs) were available for USGS gage 07105490, spanning May 1992 to September 2021. The field measurements and the rating curve for the gage are shown in Figure 2.4. Measurements with a rating of "Poor" and "Unspecified" were not included in the specific gage analysis. In addition, measured discharges exceeding 1.42 cms (50 cfs) were not included in the specific gage analysis because only six field measurements in this range were collected. The remaining 225 stage-discharge measurements were used. Because the majority of the stage-discharge data pairs corresponded to low discharge values, a smaller class size was used for low discharge measurements to evaluate changes in stage.

The results of the specific gage analysis are shown in Figure 2.5. Aggradation occurred in the channel following flood events in 1997 and 2013. In addition, in stage increases occurred after the bridge replacement in 2016 (indicated by vertical dashed lines in the figure), which may indicate regrading of the channel near the gage. While the long-term average discharge-stage relationship does not appear to have changed during the period of record, shorter cycles of aggradation and degradation after flood events are evident.

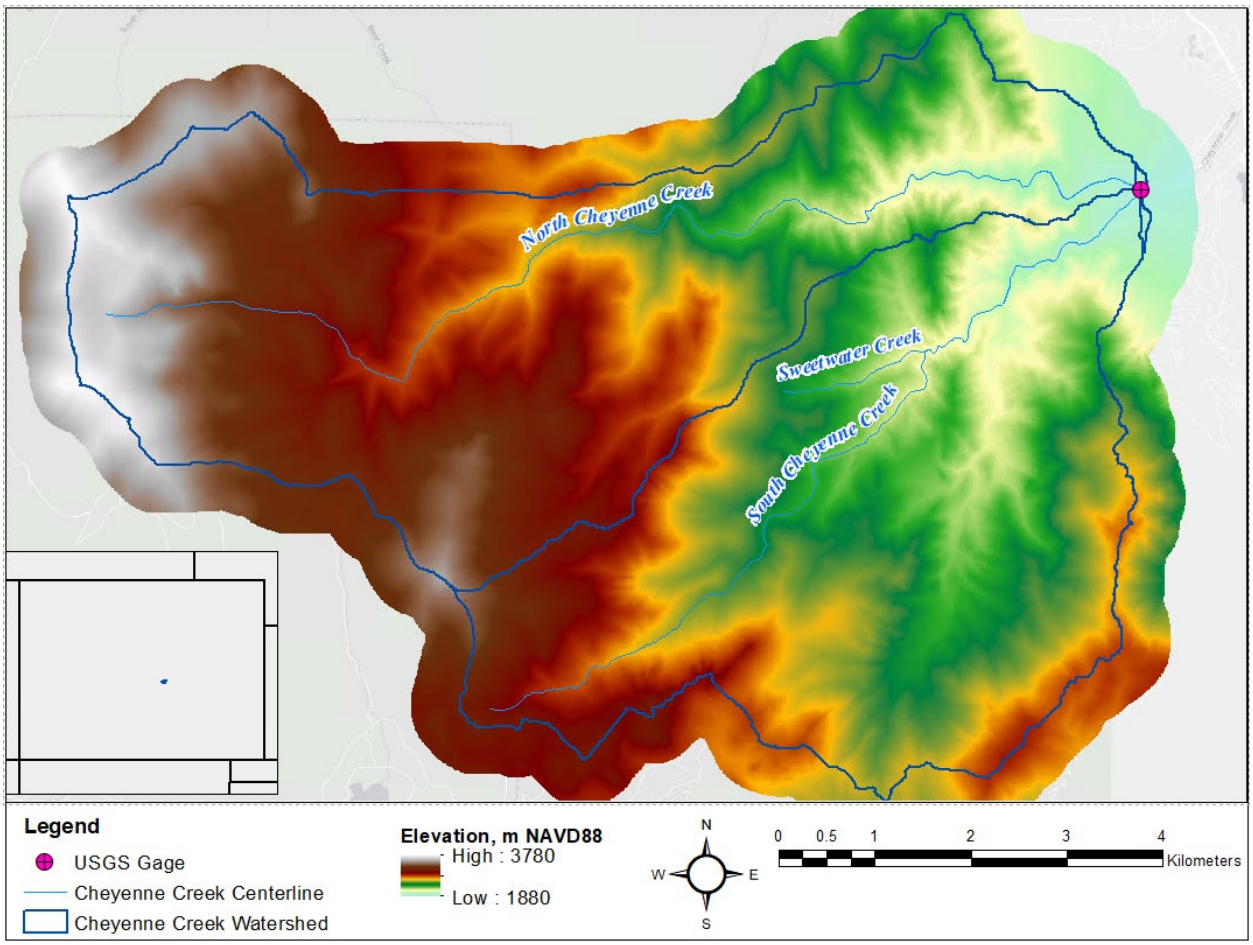

Figure 2.1 Cheyenne Creek Watershed Location and Topography

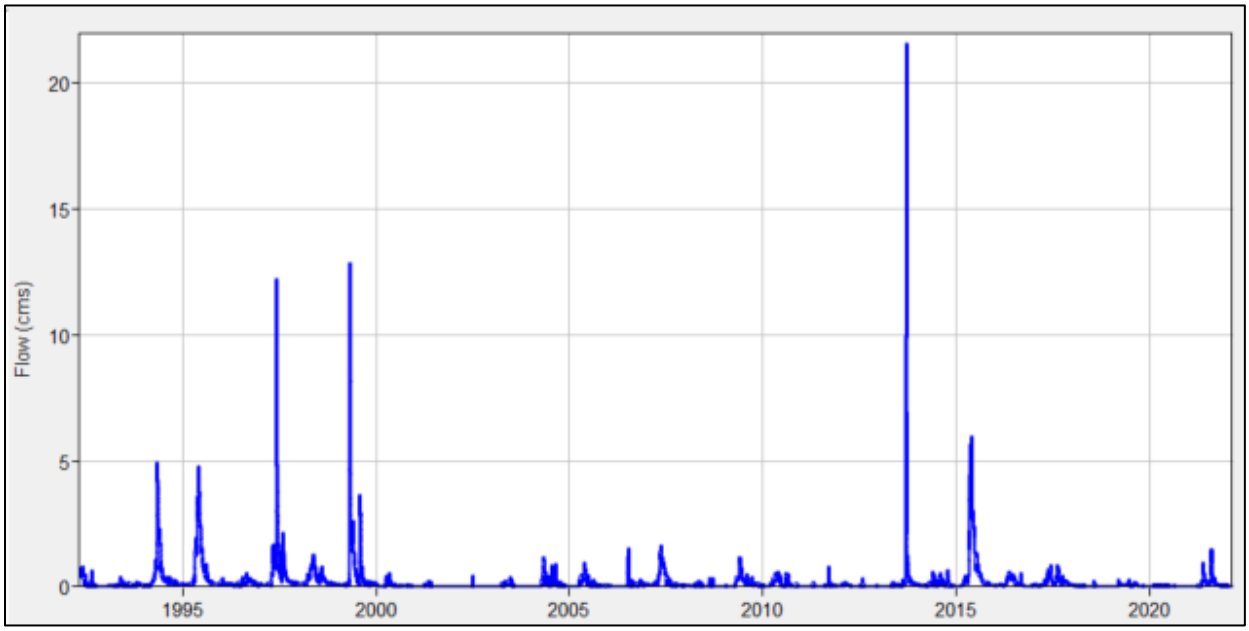

Figure 2.2 Daily Streamflow Record for USGS 07105490 Cheyenne Creek at Evans Avenue, Colorado Springs, CO

Figure 2.3 Aerial Image of Evans Avenue and South Cheyenne Canyon Road Bridges (Background Imagery from Google)

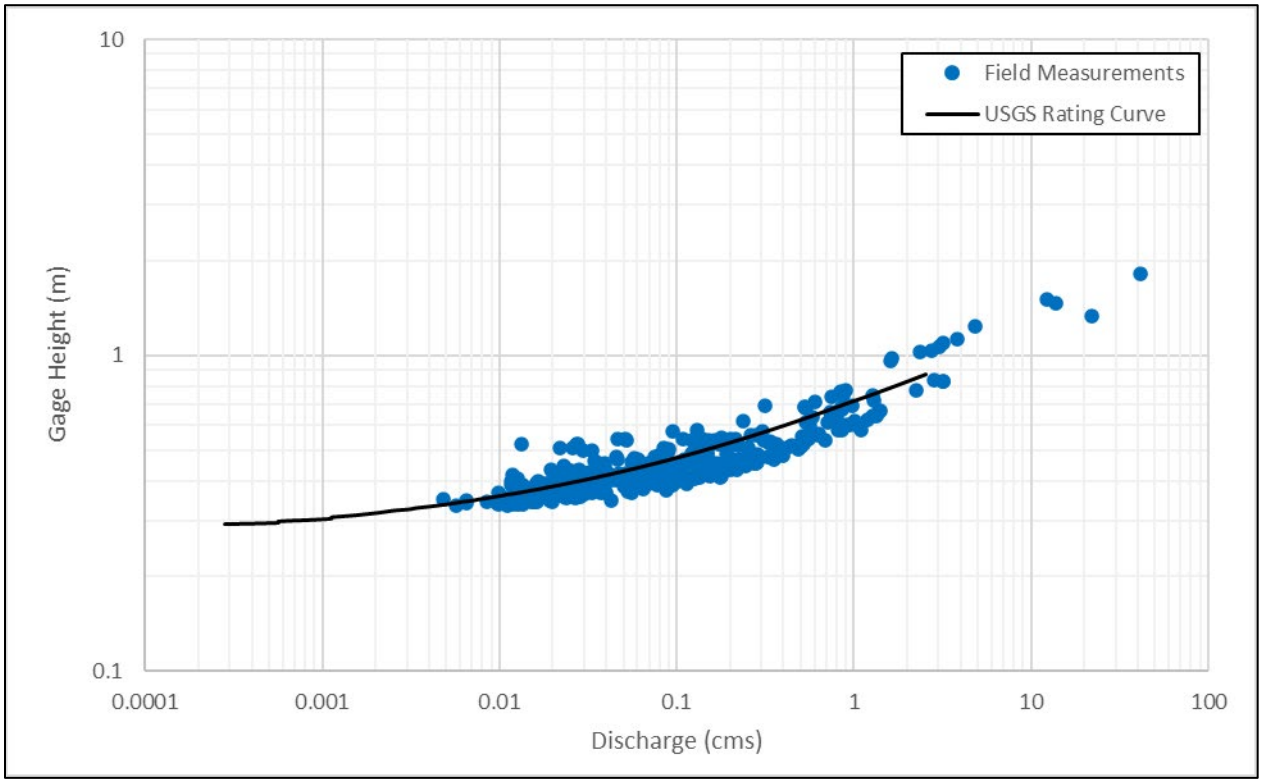

Figure 2.4 USGS Rating Curve and Field Measurements at Gage 07105490 Cheyenne Creek at Evans Avenue, Colorado Springs, CO

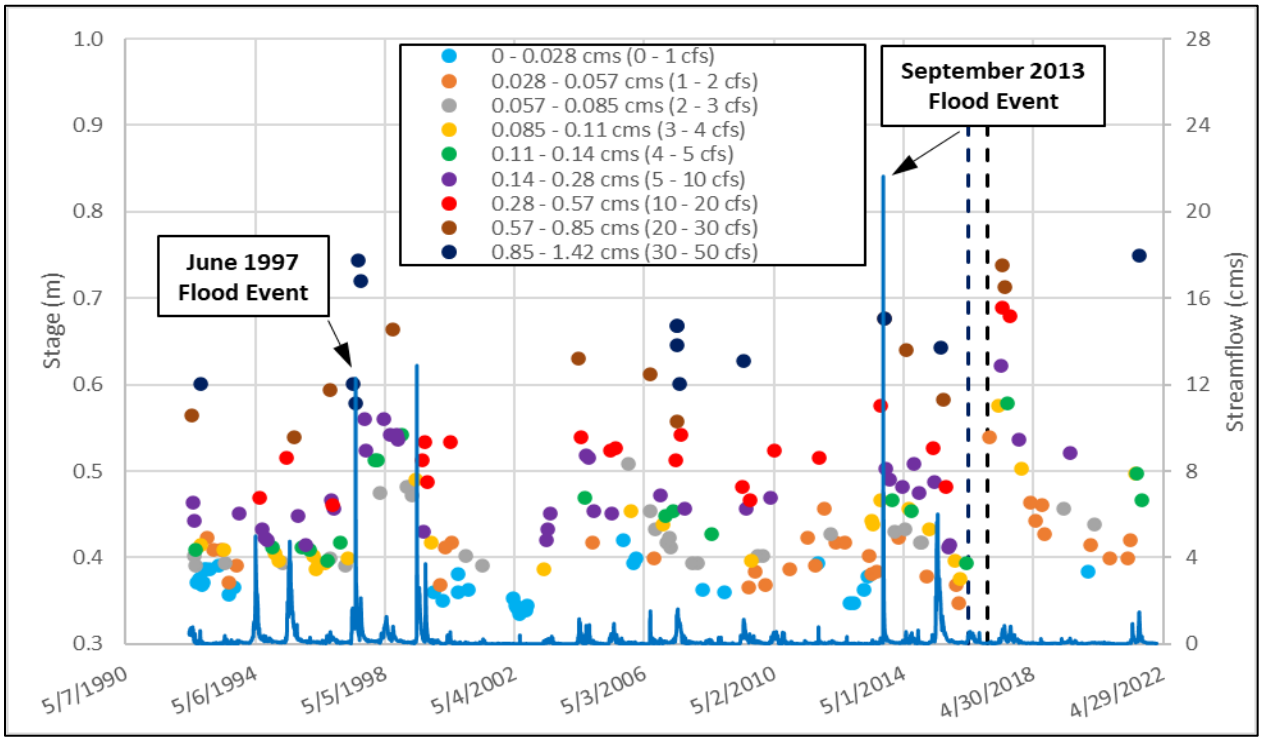

Figure 2.5 Specific Gage Analysis for Gage 07105490 Cheyenne Creek at Evans Avenue, Colorado Springs, CO

3. MODELING METHODOLOGY

3.1 Hydrologic Modeling

3.1.1 Watershed Model

HEC-HMS hydrologic models of the Cheyenne Creek watershed are available from previous research (Woolridge et al., 2020; Irvin, 2021). Woolridge et al. (2020) investigated the streamflow production mechanisms that are active during large historical storms and design storms in the Colorado Front Range. Irvin (2021) proposed parameter estimation methods to simulate infiltration-excess and saturation-excess streamflow for dam safety applications using basins in the Front Range and San Juan Range. Two versions of the model are available for Cheyenne Creek: (1) model parameters calibrated to historical storms in June 1997 and September 2013 (Woolridge et al., 2020), and (2) model parameters estimated from regional data and regression relationships (Irvin, 2021). The uncalibrated hydrologic model from Irvin (2021) was used for this project because streamflow gages are typically not available for calibration. Thus, the uncalibrated model results are more representative of typical scour analyses.

The model is semi-distributed model with three sub-basins delineated using a 15 km^2 contributing area threshold (Woolridge et al., 2020). Within the model, water can be held in canopy, soil, and groundwater storage elements. The canopy storage represents interception. All precipitation is intercepted until reaching a specified maximum canopy storage. Intercepted water is removed from the canopy by a specified evaporation rate. Precipitation that is not intercepted reaches the soil surface. The amount of water entering the soil is determined by the infiltration capacity of the soil and the remaining water is runoff. Runoff is converted to streamflow at the subbasin outlet using the Clark method. Water entering the soil is held in tension or gravity storage. Gravity storage is depleted by both evapotranspiration and gravity drainage, while tension storage is only depleted by evapotranspiration. Gravity drainage from the soil layer enters the groundwater layer. Outflow from the groundwater layer is subsurface stormflow and is routed through a linear reservoir to represent storage effects before exiting the system. Muskingum-Cunge river routing transfers flows through channels and is used to combine flow from multiple subbasins. See Woolridge et al. (2020) and Irvin (2021) for additional details about the model structure.

Parameter estimation is described in detail by Irvin (2021). The canopy evaporation rate was set to the potential evapotranspiration rate at the average subbasin elevation. Soil layer parameters were obtained from the National Resources Conservation Service (NRCS) gridded National Soil Survey Geographic database (gNATSGO). The Clark method requires a time of concentration and a linear reservoir time constant. The uncalibrated HEC-HMS model developed by Irvin (2021) uses the same Clark parameter values irrespective of the excess precipitation rate. The Clark method's uncalibrated time of concentration was obtained from an empirical relationship from Sabol (2008). Irvin (2021) proposed a storage coefficient of seven hours. Groundwater layer parameters were set to fixed values as specified by Irvin (2021). The Muskingum-Cunge method requires specification of channel length, channel slope, bed roughness, floodplain roughness, index flow, and cross-section geometry. The geometric values were obtained from satellite imagery and a digital elevation model (DEM). A rectangular cross section shape was assumed and the USGS StreamStats two-year peak streamflow was used as the index flow. The channel depth was calculated from the two-year peak streamflow and Manning's equation.

3.1.2 Variable Clark Unit Hydrograph Parameters

The variable Clark transform method in HEC-HMS was used to simulate the nonlinear relationship between excess precipitation and direct runoff. The Clark method's time of concentration and storage coefficient can vary with the excess rainfall intensity. Thus, the different excess precipitation intensities that occur during a simulation can have different values for these parameters and thus different responses. The user specifies an index excess precipitation rate along with an associated index time of concentration and index storage coefficient. The user then provides a table where each row includes the excess precipitation, time of concentration, and storage coefficient as percentages of the index values. This table defines the relationship between excess precipitation and the Clark parameters.

This relationship was determined using Colorado Dam Safety's "Guidelines for Hydrological Modeling and Flood Analysis" dated 28 March 2022 (Office of the State Engineer, Dam Safety Branch, 2022). Two peak streamflow values were used to define the relationship between the Clark parameters and the excess rainfall intensity: (1) the 1% annual exceedance probability (AEP), and (2) the Probable Maximum Flood (PMF). Estimates were obtained for these two discharges that are independent of the HEC-HMS modeling, and the Clark parameters were set to reproduce those discharge estimates.

The independent estimate of the 1% AEP discharge was obtained from StreamStats (Capesius & Stephens, 2009). The 1% AEP discharge from HEC-HMS was estimated as follows. The 1% AEP design storms with different durations were obtained from the Colorado and New Mexico Regional Extreme Precipitation Study (REPS) (The Colorado Division of Water Resources, Dam Safety Branch and the New Mexico Office of the State Engineer, Dam Safety Bureau, 2018). The storms were used in the HEC-HMS model, and the storm duration that produced the highest peak streamflow was selected for further consideration. Under an assumption of AEP neutrality, the peak streamflow produced by the selected 1% AEP design storm was compared to the 1% AEP discharge from StreamStats. This comparison neglects the role of snowmelt. The StreamStats 1% AEP peak flow is likely produced by a combination of rainfall and snowmelt (Jarrett and Tomlinson, 2000), while the uncalibrated model does not include snowmelt.

The independent PMF estimate was obtained from the regional peak flow envelope curves provided in the Colorado Dam Safety hydrologic guidelines, which are based on the USGS Colorado Flood Database. The state is divided into three climatic/geographic regions. With elevations ranging from 1,900 to 3,600 m, Cheyenne Creek straddles the Mountain (above 2,300 m elevation) and Front Range foothills (below 2,300 m elevation) regions. For a drainage area of 56 km^2, the peak envelope discharges for the Mountain and Front Range foothill regions are 156 cms and 1,784 cms, respectively. Based on recommendations from Colorado Dam Safety, a factor of safety of 1.5 was applied to the Mountain region peak discharge, resulting in a PMF of 234 cms. Probable maximum precipitation (PMP) storms were then obtained from REPS and used in the HEC-HMS model. The PMP duration that produces the largest peak flow was selected, and its peak flow was compared to the PMF from the peak envelope curve. The independent estimates of the 1% AEP and PMF discharges are shown in Table 3.1. The two-hour duration precipitation events were selected because they produced the maximum discharges.

The uncalibrated Clark parameters need to be multiplied by 75% and 9% to reproduce the independent estimates of the 1% AEP discharge and PMF, respectively. The largest excess precipitation rate from the 1% AEP event was used as the index excess precipitation rate (4.57 mm/hr for Subbasin 1, 8.06 mm/hr for Subbasin 2, and 8.84 mm/hr for Subbasin 3). The index time of concentration and storage coefficient were set to 75% of the uncalibrated values. For 100% of the index excess precipitation rate, a value of 100% was then applied to the Clark parameters. At an excess precipitation rate equivalent to the most extreme hour of the PMP event (1,674% to 3,063% of the index precipitation for the three subbasins), a value of 9% was applied to the Clark parameters. The Clark parameters and percentage curves are shown in Table 3.2 and Table 3.3, respectively.

3.2 Hydraulic Modeling

3.2.1 Physiography

Topographic data used to develop the HEC-RAS model consisted of a 2018 Colorado statewide light detection and ranging (LiDAR) dataset with a spatial resolution of 0.6 m. The horizontal datum used for this study was North American Datum of 1983 (NAD83) with the Universal Transverse Mercator (UTM) 13 North projection in meters. The vertical datum for this study was North American Vertical Datum of 1988 (NAVD88) in meters.

The North and South Cheyenne Creek streambeds are steep, ranging from 8%–10% slopes near the headwaters to 3%–4% slopes near the USGS gage. The LiDAR dataset was reconditioned along North Cheyenne Creek to improve model stability. In particular, the original LiDAR elevations contained the South Cheyenne Canyon Road bridge deck and an elevated ridge at the downstream end of North Cheyenne Creek. In the reconditioning, the North Cheyenne Creek channel bed was assumed to slope linearly from the upstream end of the modeling domain to the confluence with the south tributary. The original and reconditioned LiDAR datasets are shown in Figure 3.1 and Figure 3.2, respectively.

3.2.2 Model Structure

A two-dimensional model of Cheyenne Creek was constructed in the region of interest because Evans Avenue bridge is located directly downstream of the confluence of the North and South Cheyenne Creek tributaries, resulting in complex flow patterns. The model spans the confluence of the North and South Cheyenne Creeks with the main stem Cheyenne Creek. The hydraulic model was used to compute flow velocities and depths in the main stem of Cheyenne Creek upstream of the Evans Avenue bridge.

Two-dimensional unsteady flow routing was performed using the shallow water equations. The Navier-Stokes equations, which describe the motion of fluids in three dimensions, are simplified to the shallow water equations through the following assumptions: (1) flow is incompressible, (2) the pressure distribution is hydrostatic, (3) vertical acceleration is negligible, and (4) eddy viscosity approximates turbulent motion (Vreugdenhil, 1994). The two-dimensional flow component of HEC-RAS uses an implicit finite volume algorithm (Hydrologic Engineering Center, 2022). Cross-sectional averaged values of depth and velocity were used in the scour computations because the FHWA's current equations do not consider two-dimensional hydraulic results.

The grid cell size was selected using the Courant-Friedrichs-Lewy condition as a numerical stability criterion. This condition, commonly referred to as the Courant condition, is used to achieve convergence while solving partial differential equations (Courant et al., 1967). The condition relates the time step, spatial interval, and maximum speed of a fluid through advection. The Courant condition is calculated as:

$$C = \frac{V_w \Delta t}{\Delta x}$$

where C is the Courant number, V_w is the flood wave celerity (m/s), Δt is the computational time step (s), and Δx is the computational cell size (m) (Federal Highway Administration, 2019). An initial grid cell size was determined based on fitting five grid cells within the channel to simulate the variation in hydraulic parameters across the channel.

The FHWA recommends the use of unstructured meshes for bridge hydraulic analysis and design to allow detailed representation the flow field around structures such as piers (Federal Highway Administration, 2019). An initial two-dimensional mesh was generated, with a total of 1,800 cells, measuring 3 m by 3 m. In HEC-RAS, breaklines are geometric elements used to enforce cell faces along linear features. Breaklines were used to refine the direction of mesh cells, which in turn direct the movement of water

through the modeling domain. Breaklines were used along roadways, stream banklines, and along the channel centerline. The cell size within the channel was refined to 2 m by 2 m using the near spacing and new repeats properties of Breaklines. The final mesh configuration is shown in Figure 3.3.

The mesh has three boundary conditions (two upstream and one downstream). The upstream boundary conditions are located along the tributaries, North Cheyenne Creek and South Cheyenne Creek. The North Cheyenne Creek boundary condition line is located 50 m upstream of the confluence with the main stem of Cheyenne Creek. The South Cheyenne Creek boundary condition line is located 30 m upstream of the confluence with the main stem of Cheyenne Creek. Two upstream boundary condition lines were used to simulate the interaction of flow from the tributaries upstream of Evans Avenue bridge. The downstream boundary condition is located 110 m downstream of the confluence of North and South Cheyenne Creek with the main stem. Normal depth was assigned to the downstream boundary condition because no other USGS gages are located on Cheyenne Creek downstream of Evans Avenue bridge. As a result, neither a stage time series nor a rating curve could be specified as a downstream boundary condition. A sensitivity analysis of the downstream boundary condition location was performed to ensure that no backwater effects influenced the study area.

Two bridges cross the creek within the modeling domain. South Cheyenne Canyon Road crosses North Cheyenne Creek 30 m upstream of the confluence with the main stem. Evans Avenue crosses the main stem of Cheyenne Creek 15 m downstream of the tributary confluence. Schematics of the bridge geometry and historic streambed elevation plots were provided by CDOT and the City of Colorado Springs. The streambed elevation data were used to recondition the DEM in the vicinity of the bridges. No survey data were available in the vicinity of the bridges.

Manning's roughness values for the floodplain and river channel were assigned based on channel bed material, stream geometry, vegetation heights, structures, and land cover types (Barnes, 1967; Chow, 1959). Land cover types were obtained from the 2019 National Land Cover Dataset (Dewitz & U.S. Geological Survey, 2021). The Manning's roughness value for the channel was determined using Google Earth aerial imagery and inspection photographs provided by CDOT and the City of Colorado Springs. A Manning's roughness of 0.055 was selected for the river channel. Manning's roughness values used in the HEC-RAS model are shown in Table 3.4.

3.2.3 Sensitivity Analyses

Five sensitivity analyses were performed to test the sensitivity to model assumptions and to ensure model stability. Unless otherwise indicated, the sensitivity analyses were performed using a steady discharge of 2 cms applied to each tributary boundary condition. The combined discharge of 4 cms corresponds to the USGS StreamStats two-year peak streamflow. The sensitivity analyses were:

(1) Application of discharge as steady flow
(2) Application of discharge as unsteady flow (0 cms to 2 cms over a 2-hr period)
(3) Use of diffusion wave equations instead of shallow water equations
(4) Increase of downstream boundary condition friction slope from 0.03 to 0.05
(5) Increase of channel Manning's roughness value from 0.055 to 0.070

The average stage and velocity in the channel at USGS gage 07105490 for each sensitivity analysis are shown in Table 3.5. While the model is relatively insensitive to the changes, the shallow water equations were selected for all simulations to capture detailed velocity and water surface elevations around the bridge structure. In addition, a downstream boundary condition friction slope of 0.03 was used for all bridge scour simulations because the increased friction slope produced only a slight increase in the stage and 0.03 is similar to the channel bed slope (3%). A Manning's roughness of 0.055 was selected because

this value produced stages within the range of historical values for a combined flow of 4 cms. The increased Manning's roughness value of 0.070 only produced a slight increase in the stage.

3.3 Scour Evaluation

Two types of scour are considered in the modeling analysis: contraction scour at the bridge structure and local scour at the pier and abutments (Federal Highway Administration, 2012).

3.3.1 Contraction Scour

The critical velocity of the streambed material was calculated to determine whether the flow conditions in the channel are live-bed or clear water. If the computed average flow velocity in the channel exceeds the critical velocity for the streambed sediment, then live-bed conditions exist. Live-bed scour indicates that bed material from the upstream reach is transported into the bridge crossing.

Contraction scour computations are typically divided for the left and right overbanks and the main channel. Discharges in the upstream and contracted channel sections vary as flow enters the overbanks. In this study, only main channel contraction scour was computed.

The critical velocity (v_c in m/s) of the streambed material can be calculated using the following equation (Federal Highway Administration, 2019):

$$v_c = 6.19 y^{1/6} {D_{50}}^{1/3}$$

where y is the average depth of flow upstream of the bridge (m) and D_{50} is the median grain size (m).

In the absence of bed samples from Cheyenne Creek, a D_{50} of 1.5 mm (very coarse sand) was selected based on bed material data from nearby creeks: Sand, Monument, and Fountain (Guerard, 1989; Stogner et al., 2013). Because the computed velocities in all simulations exceed the critical velocity for a median grain size of 1.5 mm, live-bed conditions exist in the channel. However, contraction scour under live-bed conditions may be limited by armoring of the streambed by large sediment particles in the bed material (Federal Highway Administration, 2019). Because the Cheyenne Creek streambed is armored with median diameter riprap of approximately 1 m, contraction scour under both clear-water and live-bed conditions was calculated.

Live-bed contraction scour was calculated using the following equations (Federal Highway Administration, 2019):

$$y_2 = y_1 \left(\frac{Q_2}{Q_1}\right)^{6/7} \left(\frac{W_1}{W_2}\right)^{k_1}$$

$$y_s = y_2 - y_0$$

where y_1 is the average depth in the upstream main channel (m), y_2 is the average depth in the contracted section after scour has occurred (m), y_0 is the existing depth in the contracted section before scour (m), y_s is the scour depth (m), $Q_1$is the flow in the upstream channel transporting sediment (cms), Q_2 is the flow in the contracted channel (cms), W_1 is the bottom width of the upstream main channel that is transporting bed material (m), W_2 is the bottom width of the main channel in the contracted section less pier width(s) (m), and k_1 is an exponent determined from the mode of bed material transport (contact and suspended) using the ratio of the shear velocity of the upstream section to the fall velocity of the bed material (dimensionless) and is obtained from HEC-18. ;.

Clear-water contraction scour was calculated using the following equations (Federal Highway Administration, 2019):

$$y_2 = \left[\frac{0.025Q^2}{{D_m}^{2/3}{W_2}^2}\right]^{3/7}$$

$$y_s = y_2 - y_0$$

where Q is the discharge through the bridge associated with the width W, D_m is the diameter of the smallest non-transportable particle in the bed material ($1.25D_{50}$ based on the assumption that the scoured section is armored), and W_2 is the bottom width of the contracted section less the pier width.

3.3.2 Pier Scour

Scour around bridge piers is a function of the streambed geometry, flow characteristics, bridge substructure geometry, and the bed material (Federal Highway Administration, 2012). The pier scour equation in HEC-18 was developed based on field measurements. The equation frequently overpredicts observed scour depths (Federal Highway Administration, 2012). The pier scour equation predicts maximum scour depths under both live-bed and clear-water conditions. The original Evans Avenue bridge design had a single centrally located square-nose pier. Scour depths are amplified by the orientation of the main stem Cheyenne Creek with respect to the bridge pier. The angle of attack of the flow is approximately 23°.

Pier scour is calculated using the following equation (Federal Highway Administration, 2012):

$$\frac{y_s}{y_1} = 2.0\, K_1\, K_2\, K_3 \left(\frac{a}{y_1}\right)^{0.65} {Fr_1}^{0.43}$$

where y_1 is the flow depth directly upstream of the pier (m), y_s is the scour depth (m), K_1 is a correction factor for the pier nose shape (dimensionless), K_2 is a correction factor for the angle of attack of the flow (dimensionless), K_3 is a correction factor for the bed condition (dimensionless), a is the pier width (m), and Fr_1 is the Froude number directly upstream of the pier (dimensionless).

The values for the correction factors K_1, K_2, and K_3 are provided in HEC-18. The correction factor for the pier nose shape K_1 varies from 0.9 for sharp nose piers to 1.1 for square nose piers. A value of 1.1 was used because the Evans Avenue bridge had a single square nose pier. The correction factor for the angle of attack of flow K_2 is calculated using the following equation:

$$K_2 = (\cos\theta + \frac{L}{a}\sin\theta)^{0.65}$$

where θ is the angle of attack of flow (degrees), L is the length of the pier (m), and a is the pier width (m). The K_2 correction factor has a maximum value of 5.0, and a value of 3.0 was used in this study. The correction factor for the bed condition K_3 varies from 1.1 for clear water scour to 1.3 for large dunes (greater than 30 feet in height). A K_3 value of 1.1 was used in this study.

3.4 Simulations

3.4.1 Hydrologic Model Simulations

Hydrologic simulations were performed using constant Clark parameters, which neglect the nonlinear response of watersheds, and the variable Clark parameters, which include the nonlinearity. For both

approaches, simulations were conducted for two-hour duration design storms with AEPs ranging from 1% to 0.00001% (10^{-2}-yr to 10^{-7}-yr). The design storms were generated based on the Colorado and New Mexico REPS (The Colorado Division of Water Resources, Dam Safety Branch and The New Mexico Office of the State Engineer, Dam Safety Bureau, 2018). All model simulations utilized canopy, loss, baseflow, and reach routing parameters described in Section 3.1.1. The results were used in the hydraulic model to compute channel depth and velocity.

3.4.2 Hydraulic Model Simulations

Hydraulic model simulations and scour calculations were performed only for larger AEPs, which satisfy FHWA recommendations (Federal Highway Administration, 2012). The discharges were obtained from three different approaches. The first approach uses peak flow rates from StreamStats (AEPs of 2%, 1%, 0.5%, and 0.2%) and applies those flow rates as steady flows for three hours because the shape of the hydrograph from StreamStats is not known. By using a single streamflow, this approach neglects the impact that flow variations have on the hydraulics and scour. The second approach uses streamflow hydrographs obtained using the constant Clark parameters (AEPs of 1%, 0.1%, and 0.01%). This approach includes flow variations but neglects the nonlinear response of the watershed. The third approach uses streamflow hydrographs from the variable Clark parameters (AEPs of 1%, 0.1%, and 0.01%). This approach includes both flow variations and the nonlinear response of the watershed.

Table 3.1 Independent Estimates of Peak Flow

Design Storm	Source	Peak Flow (cms)
1% AEP	StreamStats	17.3
PMP	Regional Peak Flow Envelope (Mountain Region)	234
PMP	Regional Peak Flow Envelope (Front Range Foothills Region)	1,784

Table 3.2 Uncalibrated and Calibrated Clark Parameters for Front Range Foothills Region

Subbasin	Uncalibrated		Calibrated to StreamStats 1% AEP Flow		Calibrated to 2-hr PMF from Front Range Region	
	T_c (hr)	R (hr)	T_c (hr)	R (hr)	T_c (hr)	R (hr)
Multiplication Factor Applied to Uncalibrated Parameters (%)	100	100	75	75	7	7
Subbasin-1	1.87	7	1.40	5.25	0.13	0.49
Subbasin-2	1.51	7	1.13	5.25	0.11	0.49
Subbasin-3	0.36	7	0.27	5.25	0.03	0.49

T_c is Time of Concentration, R is Storage Coefficient

Table 3.3 Variable Clark Transform Parameters Percentage Curves

Subbasin-1		Subbasin-2		Subbasin-3	
Percent (%)	Percent (%)	Percent (%)	Percent (%)	Percent (%)	Percent (%)
0	100	0	100	0	100
100	100	100	100	100	100
3,063	9.3	1,824	9.3	1,674	9.3

Table 3.4 Manning's Roughness Values for Cheyenne Creek HEC-RAS Model

Land Cover	Manning's Roughness
River Channel	0.055
Developed, Open Space	0.03
Developed, Low Intensity	0.06
Developed, Medium to High Intensity	0.1
Tree Canopy (Forested)	0.1

Table 3.5 Results of Sensitivity Analyses Performed on Cheyenne Creek HEC-RAS Model

Run No.	Sensitivity Analysis	Average Stage (m)	Average Velocity (m/s)
1	Application of discharge as steady flow	0.83	0.69
2	Application of discharge as unsteady flow (0 cms to 2 cms over a 2-hour period)	0.77	0.68
3	Diffusion wave instead of shallow water equations	0.77	0.86
4	Increase downstream boundary condition friction slope from 0.03 to 0.05	0.83	0.69
5	Increased channel roughness from 0.055 to 0.070	0.77	0.79

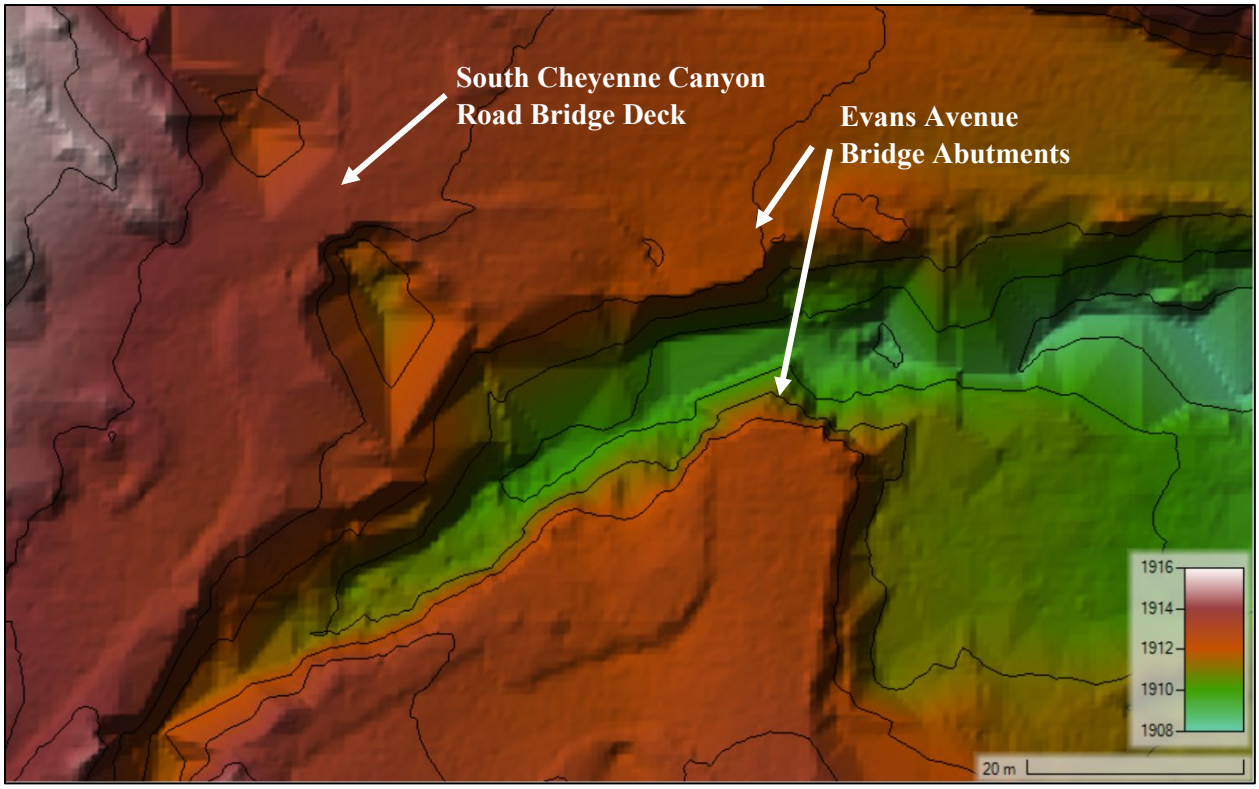

Figure 3.1 Cheyenne Creek Digital Elevation Model with 1-m Contours

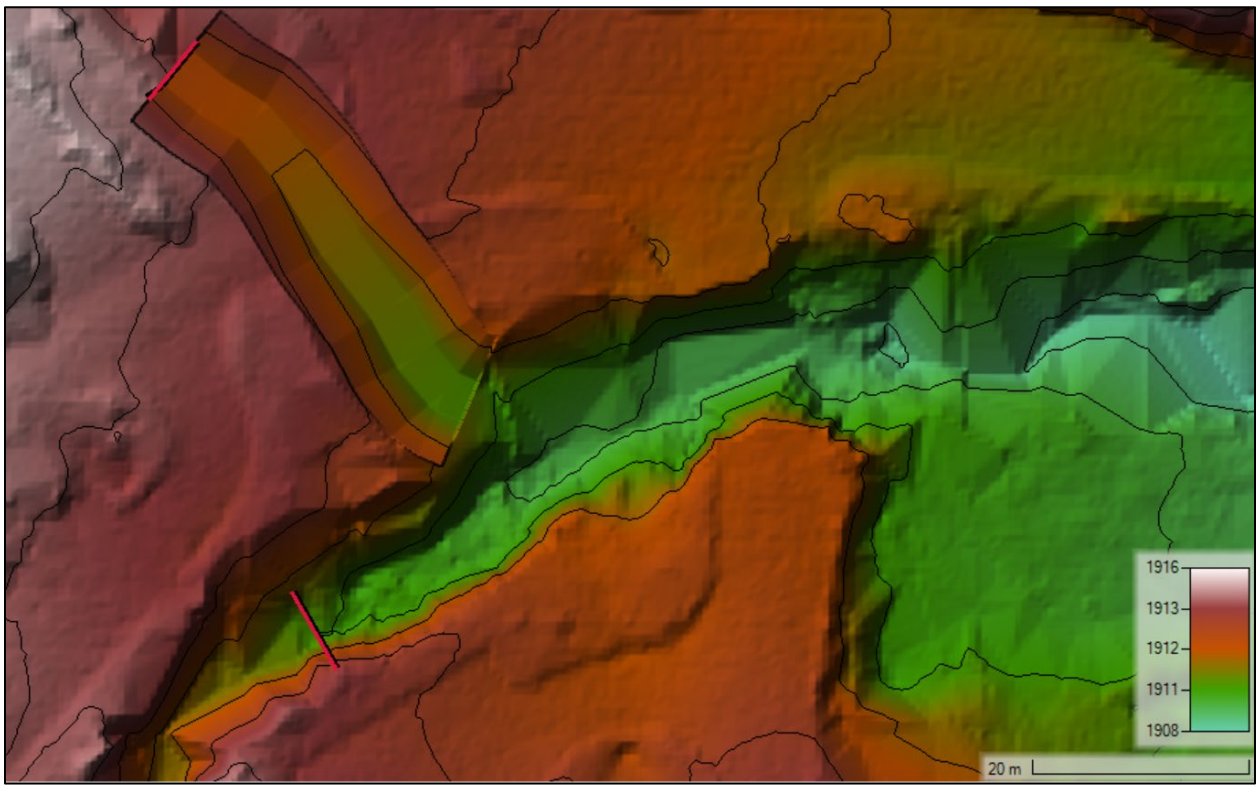

Figure 3.2 Reconditioned Cheyenne Creek Digital Elevation Model with 1-m Contours and Upstream Boundary Condition Lines

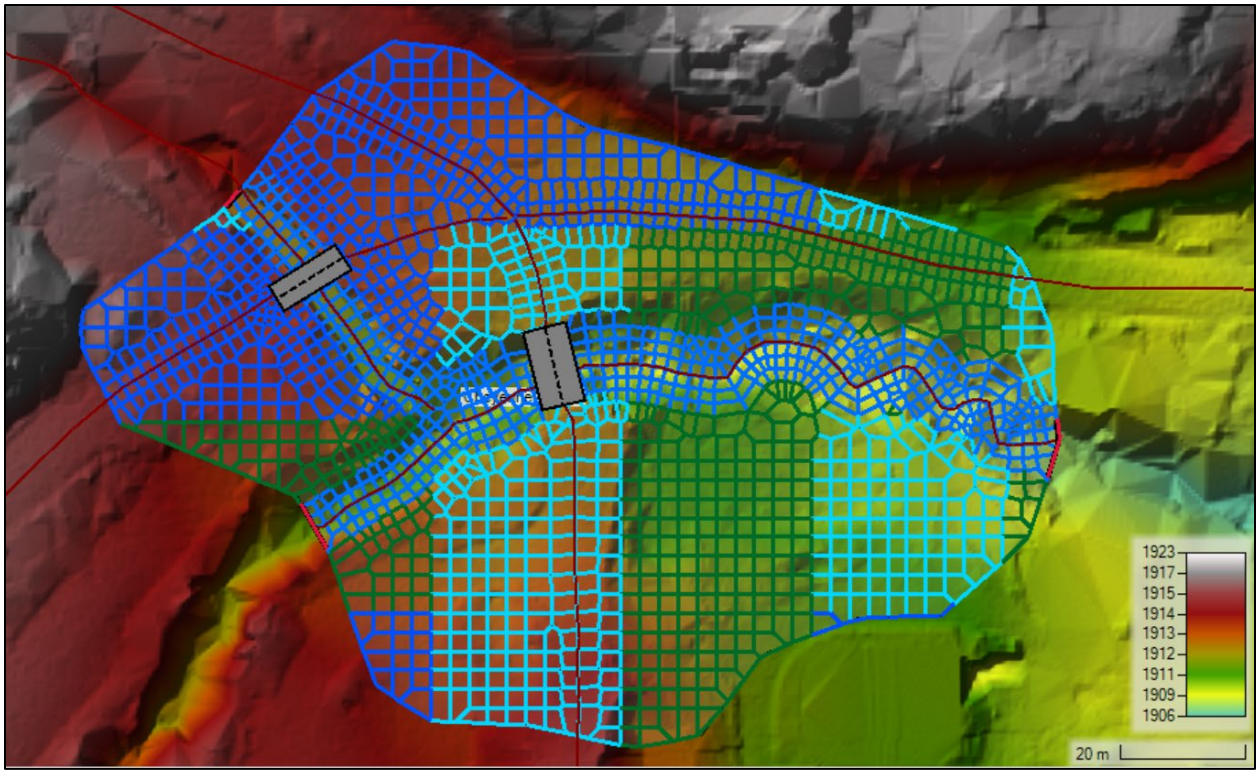

Figure 3.3 Cheyenne Creek HEC-RAS 2-Dimensional Mesh

4. RESULTS

4.1 Hydrologic Modeling Results

The simulated peak discharges from the models using constant and variable Clark parameters are shown in Table 4.1 and Figure 4.1. The discharges listed in the Variable Clark Parameters column of Table 4.1 for the 1% AEP and PMF events were calibrated to the independent flow estimates as described in the methods section. The calibrated 1% AEP and PMF discharges were 30% and 466% higher than those obtained from the uncalibrated model using constant Clark parameters. The inclusion of the variable Clark parameters increased the peak discharge across all AEPs. The increase in peak discharge was more pronounced at the smaller AEPs (i.e., rarer events). Peak discharge for the 0.1% and 0.01% AEP events increased by 58% and 84% by utilizing variable Clark parameters.

Complete hydrographs from the two approaches are shown in Figure 4.2. To reproduce the peak flows at the rarest AEPs, the Clark parameters were adjusted such that the watershed exhibits very rapid runoff response and essentially no storage at high precipitation rates. The extremely high PMF discharge from the regional peak flow envelope curve is the result of highly dynamic weather in the Front Range Foothills and rapid runoff response that is governed by the steep terrain (Office of the State Engineer, Dam Safety Branch, 2022).

4.2 Hydraulic Modeling Results

Contraction scour depths were computed in the main channel for the StreamStats flow values (given in Table 4.2) and the HEC-HMS generated hydrographs. Table 4.3 summarizes the results from the StreamStats flows, and Table 4.4 summarizes the results for the HEC-HMS flows. All the results are shown graphically in Figure 4.3. For a given AEP, the live-bed scour results were similar for all three cases. The computed clear-water contraction scour depths were significantly larger than the live-bed contraction scour depths for all simulations. Clear-water contraction scour depths were significantly larger than live-bed contraction scour depths because live-bed scour is often limited by coarse sediments in the bed material armoring the bed. Using variable flow reduces the clear-water and live-bed scour depths. At the 1% AEP, for example, the StreamStats case produces 2.29 m and 0.36 m of clear-water and live-bed scour, respectively, while the constant Clark case produces 1.93 m and 0.03 m of clear-water and live-bed scour, respectively. However, including the nonlinear response can substantially raise the scour depths. At the 1% AEP, the variable Clark cases produced similar clear-water (2.30 m) and live-bed (0.10 m) scour depths as the constant Clark case. As one considers rarer events (0.1% and 0.01%), the difference between the constant and variable Clark cases increases. Furthermore, the clear-water results from the variable Clark case become increasingly dissimilar from the StreamStats results. The differences observed in the contraction scour depths are commensurate with the differences in the peak discharges.

Results from the pier scour computations are summarized in Table 4.5 and Table 4.6 and shown graphically in Figure 4.4. Computed pier scour depths range from 2.8 to 3.8 m. Pier scour depths calculated from the StreamStats discharges are significantly higher than those computed from the constant and variable Clark hydrographs, but the constant and variable Clark cases generally produce similar pier scour depths. For example, at 1% AEP, the pier scour depth predicted for the StreamStats case is about 3.6 m, while both Clark cases produce pier scour depths around 2.7 m.

Table 4.1 Comparison of 2-hr Duration Design Storm Peak Flows (cms) from Constant and Variable Clark Parameter Simulations

AEP (%)	Constant Clark Parameters	Variable Clark Parameters	% Increase in Peak Discharge Estimate
1	13.0	16.9*	30
0.1	32.0	50.6	58
0.01	54.4	100	84
0.001	80.9	178	120
0.0001	111	232	109
0.00001	141	334	137
PMF	318	1,800*	466

*Calibrated to independent discharge estimate

Table 4.2 USGS StreamStats Peak Flow Statistics for Cheyenne Creek Watershed

AEP (%)	Return Period (years)	Discharge (cms)
2	50	14.4
1	100	17.4
0.5	200	20.5
0.2	500	26.2

Table 4.3 Live-bed and Clear-water Contraction Scour Depths for USGS StreamStats Steady Peak Flow Simulations

AEP (%)	10	2	1	0.5	0.2
Critical velocity, v_c (m/s)	0.68	0.72	0.73	0.75	0.78
Average velocity upstream of bridge (m/s)	1.12	1.36	1.47	1.59	1.79
Average live-bed contraction scour depth, y_s (m)	0.07	0.28	0.36	0.44	0.77
Average clear-water contraction scour depth, y_s (m)	1.43	1.99	2.29	2.59	3.14

Table 4.4 Live-bed and Clear-water Contraction Scour Depths for 2-hr Duration Design Hydrographs

Clark Parameters	Constant			Variable		
AEP (%)	1	0.1	0.01	1	0.1	0.01
Critical velocity, v_c (m/s)	0.72	0.80	0.83	0.74	0.83	0.85
Average velocity upstream of bridge (m/s)	1.09	1.30	1.42	1.14	1.37	1.59
Average live-bed contraction scour depth, y_s (m)	0.03	0.57	0.66	0.10	0.98	1.06
Average clear-water contraction scour depth, y_s (m)	1.93	3.53	5.71	2.30	6.17	6.83

Table 4.5 Pier Scour Depths for USGS StreamStats Steady Peak Flow Simulations

AEP (%)	10	2	1	0.5	0.2
Flow depth directly upstream of pier, y_1 (m/s)	1.40	1.73	1.84	1.95	2.17
Flow velocity directly upstream of pier, v_1 (m/s)	1.48	1.99	2.02	2.02	2.13
Pier scour depth, y_s (m)	3.03	3.55	3.60	3.63	3.76

Table 4.6 Pier Scour Depths for 2-hr Duration Design Hydrographs

Clark Parameters	Constant			Variable		
AEP (%)	1	0.1	0.01	1	0.1	0.01
Flow depth directly upstream of pier, y_1 (m/s)	0.88	1.00	3.31	1.34	2.52	2.95
Flow velocity directly upstream of pier, v_1 (m/s)	1.39	1.47	1.50	1.14	1.37	1.59
Pier scour depth, y_s (m)	2.77	2.89	3.43	2.69	3.18	3.46

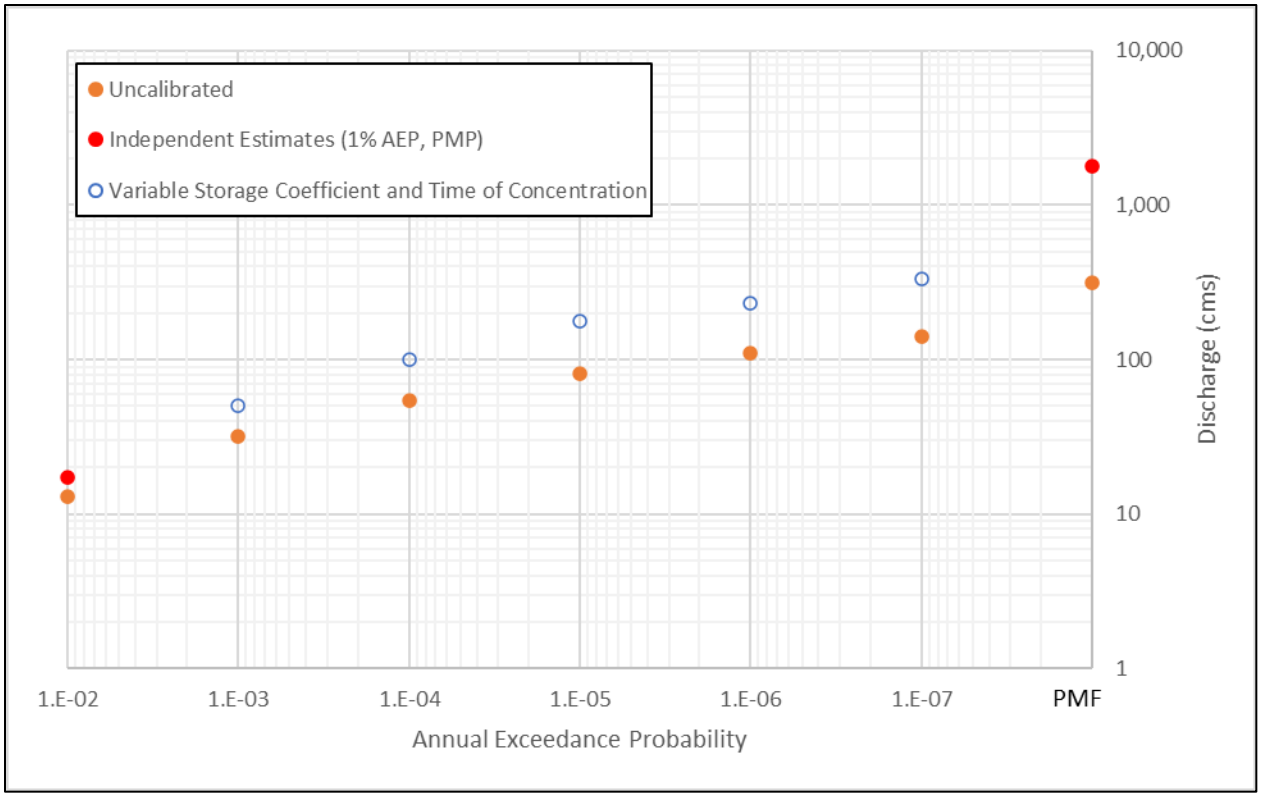

Figure 4.1 Peak Streamflow for Constant and Variable Clark Parameters

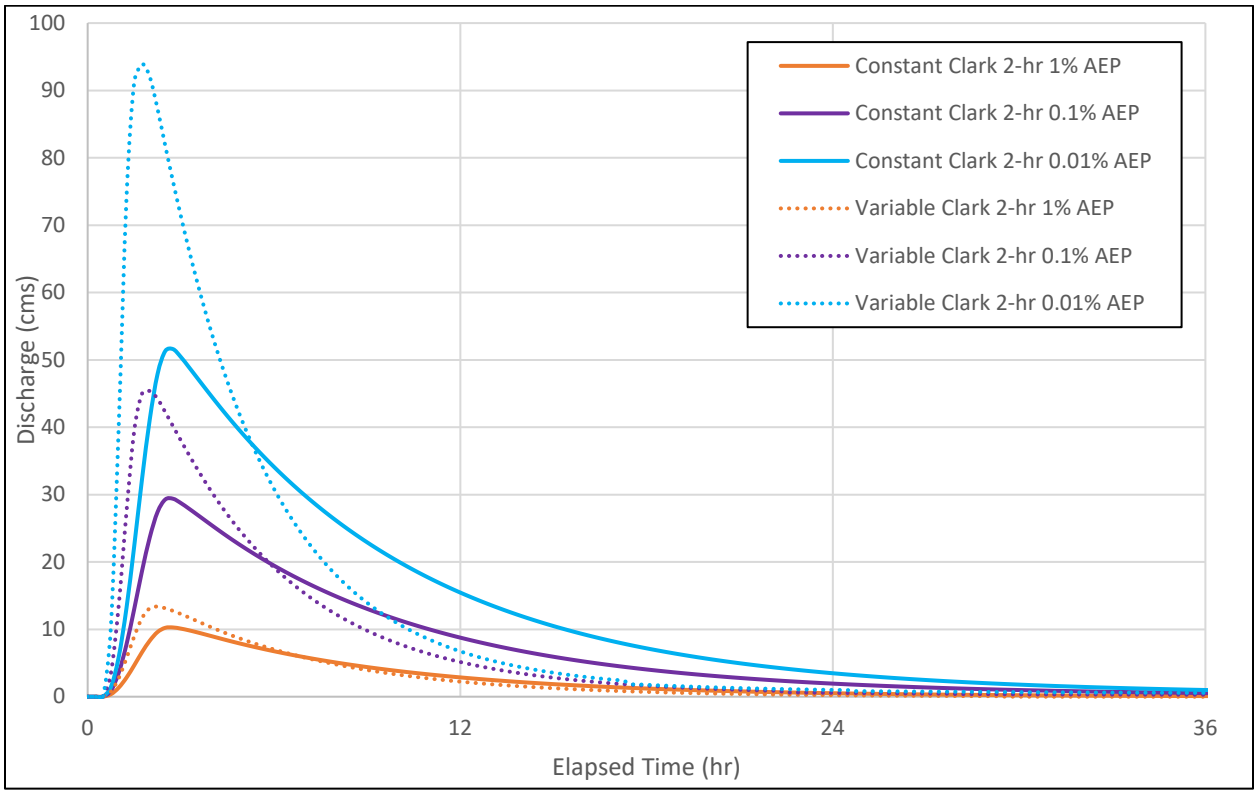

Figure 4.2 Cheyenne Creek 2-hr Design Storm Hydrographs

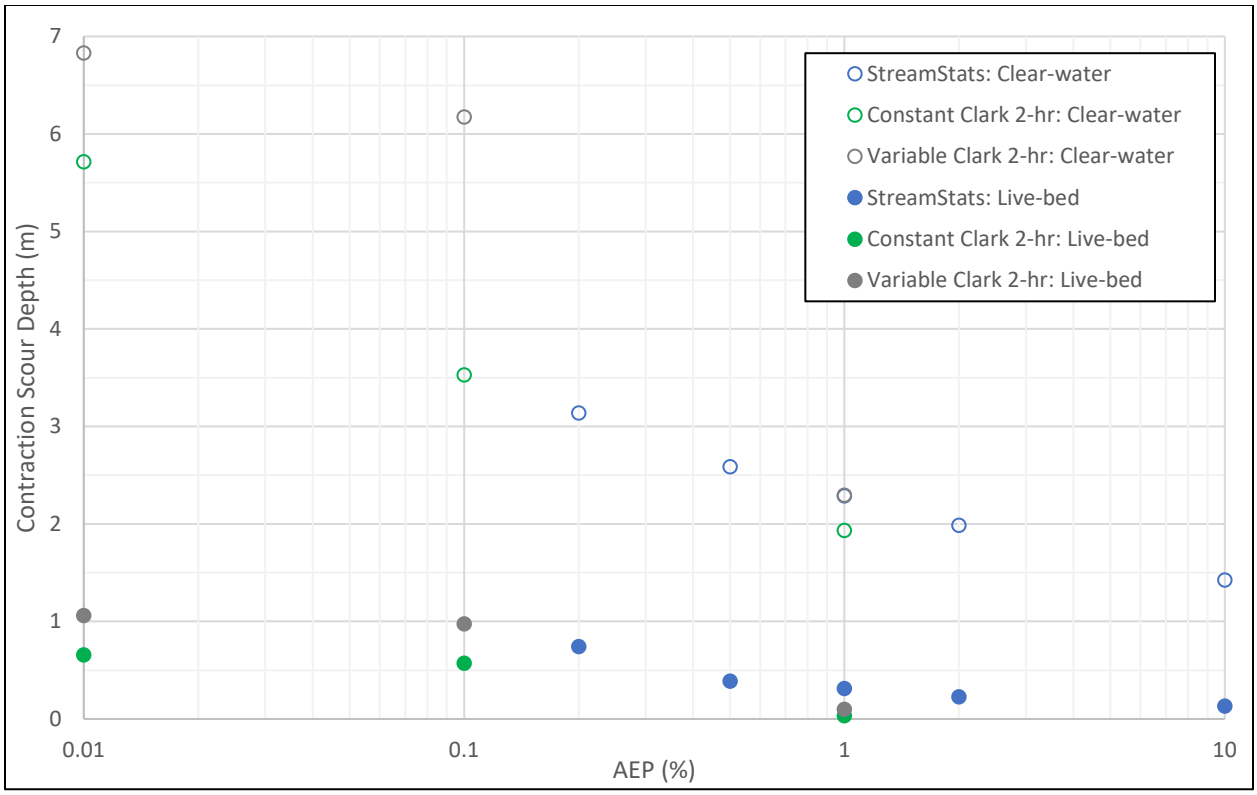

Figure 4.3 Clear-Water and Live-bed Contraction Scour Results for Evans Avenue Bridge

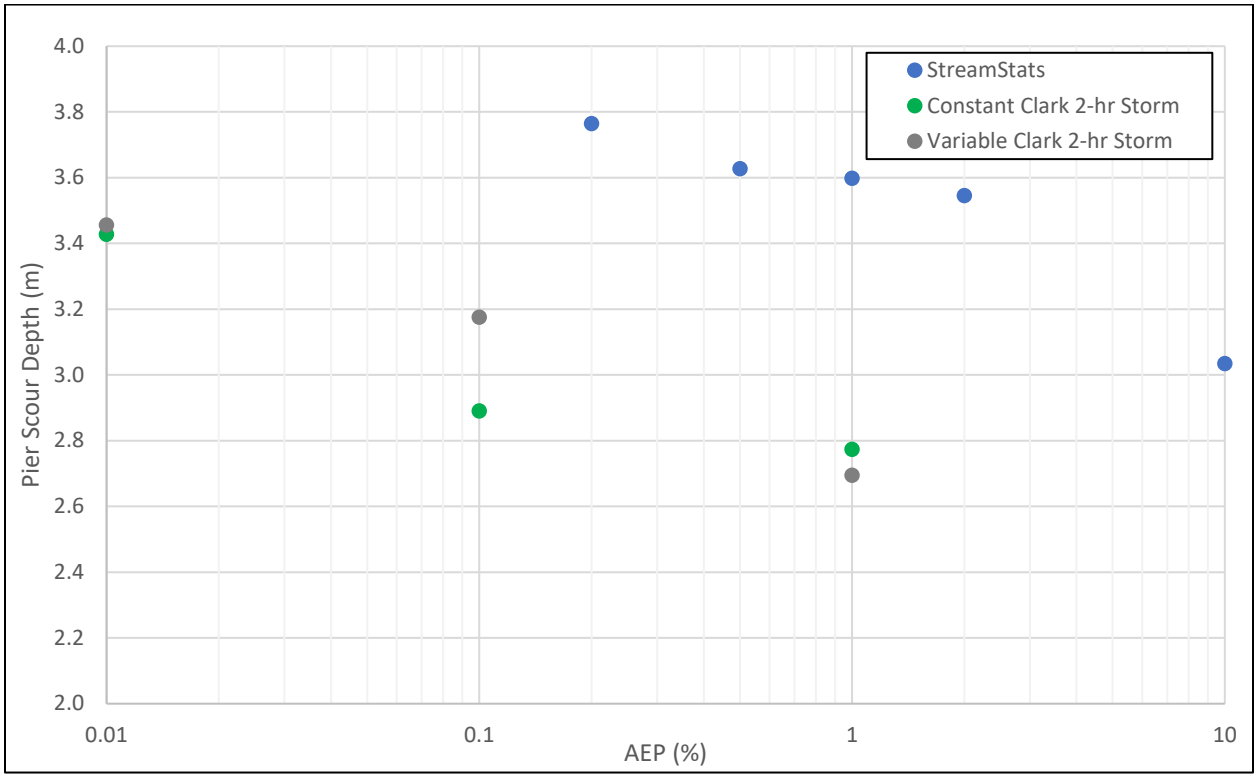

Figure 4.4 Pier Scour Results for Evans Avenue Bridge

5. CONCLUSIONS

This study aimed to investigate the impact of the nonlinear rainfall-runoff response of watersheds on bridge scour. A case study was performed using Cheyenne Creek, which is west of Colorado Springs. Streamflow values were obtained from three approaches: (1) regression equations in StreamStats, (2) an HEC-HMS model with constant Clark parameters, and (3) an HEC-HMS model with variable Clark parameters. The resulting flows were supplied to a two-dimensional HEC-RAS model, and the resulting flow depths and velocities were used in scour calculations for the Evans Avenue Bridge.
The following conclusions can be drawn from this study:

- The peak flow envelope curve presented in Colorado Dam Safety's "Guidelines for Hydrological Modeling and Flood Analysis" for the Front Range Foothills region yields extremely high PMF discharges. Observed flood discharges used to develop this curve supports the hypothesis that nonlinearity between excess precipitation rate and discharge exists in the Front Range region.
- The incorporation of a variable relationship between excess precipitation rate and Clark parameters increased the peak discharge for all AEPs. The increase in peak discharge ranged from 30% for the 1% AEP event to 466% for the PMF. These percentages depend on the calibration to the independent estimates of peak flows and are therefore expected to differ for other locations. However, a similar calibration procedure could be implemented at other locations.
- The live-bed contraction scour depths computed using steady flows from StreamStats and the unsteady simulated hydrographs were similar for all AEPs.
- For AEPs below 0.1%, the clear-water contraction scour depths were significantly higher when the variable Clark parameters were used than when the constant Clark parameters were used. This result suggests that the nonlinear response of basins becomes more important to clear-water scour when larger (rarer) events are evaluated.
- Pier scour depths computed using the StreamStats steady peak flows were higher than those computed using the unsteady simulated hydrographs of the same frequency. For example, the pier scour depth computed from the 0.2% AEP StreamStats peak flow was larger than the depth computed from the 0.01% AEP event simulated using the variable Clark method. This likely occurs due to backwater resulting from obstruction of the extremely high discharges by the bridge structures over the creek.
- Overall, pier scour depths were similar when the constant or the variable Clark parameters were used.

While these results suggest that the basin response can have substantial implications for scour, additional research is needed in several areas. First, the methods should be applied to other basins within the Colorado Front Range foothills and in other regions. Nonlinearity in the relationship between excess precipitation intensity and discharge have been observed in watersheds in the Colorado Front Range, but the extent of this nonlinear relationship has not been quantified. In addition, watersheds both within and outside of the region may behave differently because of differences in terrain and vegetation. Second, future FHWA scour design procedures will leverage two-dimensional and mobile bed modeling capabilities to better evaluate scour (Federal Highway Administration, 2019). The improved guidelines will accommodate two-dimensional hydrologic models that explicitly route excess precipitation without using unit hydrograph theory, two-dimensional hydraulic models that simulate complex flow interactions at confluences and hydraulic structures, and sediment transport models that can capture the cyclic nature of scour between flood events. The implications of basin response for these new modeling procedures should be considered. Third, the variable Clark parameters were developed using two independent estimates of frequency-based discharges. The StreamStats 1% AEP peak flow is based on multiple flood causal mechanisms (rainfall, snowmelt, rain-on-snow, etc.), whereas the hydrologic model simulates only rainfall events. Additional research is needed to develop an independent estimate of the 1% AEP event that is based solely on rainfall events.

6. REFERENCES

Amorocho, J. (1963). “Measures of the linearity of hydrologic systems.” *Journal of Geophysical Research*, *68*(8), 2237–2249. https://doi.org/10.1029/JZ068i008p02237

Barnes, Jr., H. H. (1967). "Roughness Characteristics of Natural Channels." U.S. Geological Survey, Department of the Interior. Washington, D.C.: United States Government Printing Office.

Barnes, H. H. (1967). *Roughness Characteristics of Natural Channels*. U.S. Department of the Interior, U.S. Geological Survey.

Biedenharn, D. S., & Watson, C. C. (1997). "Stage adjustment in the Lower Mississippi River," USA. *Regulated Rivers*, *13*(6), 517–536. https://doi.org/10.1002/(SICI)1099-1646(199711/12)13:6<517::AID-RRR482>3.0.CO;2-2

Blench, T. (1969). *Mobile-Bed Fluviology A Regime Theory Treatment of Canals and Rivers for Engineers and Hydrologists*. The University of Alberta Press.

Capesius, J. P., & Stephens, V. C. (2009). *Regional Regression Equations for Estimation of Natural Streamflow Statistics in Colorado* (Scientific Investigations Report 2009-5136). U.S. Geological Survey.

Chow, V. T. (1959). *Open-Channel Hydraulics* (1959 Edition Reprint). The Blackburn Press.

Clopper, P. E., & Lagasse, P. F. (2011). "Hydrologic Uncertainty in Prediction of Bridge Scour." *Transportation Research Record*, *2262*(1), 207–213. https://doi.org/10.3141/2262-21

Colorado Department of Water Resources. (n.d.). *Stations—Current and Historical*. Colorado’s Decision Support Systems. https://dwr.state.co.us/Tools/Stations

Courant, R., Friedrichs, K., & Lewy, H. (1967). "On the Partial Difference Equations Equations of Mathmatical Physics." *IBM Journal of Research and Development*, *11*(2), 215–234. https://doi.org/10.1147/rd.112.0215

Dewitz, J., & U.S. Geological Survey. (2021). *National Land Cover Database (NLCD) 2019 Products* (ver. 2.0) [Map]. U.S. Geological Survey data release. https://doi.org/10.5066/P9KZCM54

Dooge, J. C. I. (1959). "A general theory of the unit hydrograph." *Journal of Geophysical Research*, *64*(2), 241–256. https://doi.org/10.1029/JZ064i002p00241

Federal Energy Regulatory Commission. (2001). *Chapter VIII Determination of the Probable Maximum Flood, Engineering Guidelines for the Evaluation of Hydropower Projects*. FERC.

Federal Highway Administration. (2012). *Hydraulic Engineering Circular No. 18, Evaluating Scour at Bridges, FHWA HIF-12-003*. U.S. Department of Transportation.

Federal Highway Administration. (2019). *Two-Dimensional Hydraulic Modeling for Highways in the River Environment, FHWA HIF-19-061*. U.S. Department of Transportation.

Guerard, P. von. (1989). *Sediment-Transport Characteristics and Effects of Sediment Transport on Benthic Invertebrates in the Fountain Creek Drainage Basin Upstream from Widefield, Southeastern Coloardo, 1985-1988* (WRI 89-4161). U.S. Geological Survey, Department of the Interior.

Hydrologic Engineering Center. (2022). *HEC-RAS User’s Manual version 6.1*. Introduction to HEC-RAS. https://www.hec.usace.army.mil/confluence/rasdocs/rasum/latest/introduction-to-hec-ras

Irvin IV, B. C. (2021). *Parameter Estimation Methods for Models of Major Flood Events in Ungauged Mountain Basins in Colorado* (master’s thesis). Colorado State University.

Jarrett, R., & Tomlinson, E. (2000). "Regional Interdisciplinary Paleoflood Approach to Assess Extreme Flood Potential." *Water Resources Research*, *36*(10), 2957–2984. https://doi.org/doi:10.1029/2000wr900098

Lee, K. T., & Yen, B. C. (1997). "Geomorphology and Kinematic-Wave-Based Hydrograph Derivation." *Journal of Hydraulic Engineering (New York, N.Y.)*, *123*(1), 73–80. https://doi.org/10.1061/(ASCE)0733-9429(1997)123:1(73)

Mommandi, A., Yanagihara, S., & Molinas, A. (2004). *Chapter 7 Hydrology, Drainage Design Manual*. Colorado Department of Transportation.

Office of the State Engineer, Dam Safety Branch. (2022). *Guidelines for Hydrological Modeling and Flood Analysis (Draft)*. State of Colorado Department of Natural Resources, Division of Water Resources.

Stogner, Sr., R. W., Nelson, J. M., McDonald, R. R., Kinzel, P. J., & Mau, D. P. (2013). *Prediction of Suspended-Sediment Concentrations at Selected Sites in the Fountain Creek Watershed, Colorado, 2008-2009* (SIR 2012-5102). U.S. Geological Survey, Department of the Interior.

The Colorado Division of Water Resources, Dam Safety Branch and The New Mexico Office of the State Engineer, Dam Safety Bureau. (2018). *Colorado-New Mexico Regional Extreme Precipitation Study Summary Report* (Volume 1: Project Background and Overview).

Tromp-van Meerveld, H. J., & McDonnell, J. J. (2006). "Threshold relations in subsurface stormflow: 1. A 147-storm analysis of the Panola hillslope." *Water Resources Research*, *42*(2), W02410-n/a. https://doi.org/10.1029/2004WR003778

Tromp-van Meerveld, H. J., & McDonnell, J. J. (2006). "Threshold relations in subsurface stormflow: 2. The fill and spill hypothesis." *Water Resources Research*, *42*(2), W02411-n/a. https://doi.org/10.1029/2004WR003800

U.S. Army Corps of Engineers. (1991). *Inflow Design Floods for Dams and Reservoirs* (Engineer Regulation 1110-8-2). USACE.

Vreugdenhil, C. B. (1994). *Numerical Methods for Shallow-Water Flow*. Springer Netherlands. https://doi.org/10.1007/978-94-015-8354-1

Woolridge, D. D., Niemann, J. D., Perry, M. A., Bauer, K. E., & McCormick, W. T. (2020). "Identifying Runoff Production Mechanisms for Dam Safety Applications in the Colorado Front Range." *Journal of Hydrologic Engineering*, *25*(8), 5020016-. https://doi.org/10.1061/(ASCE)HE.1943-5584.0001958